Erciyes University Journal of Institue Of Science and Technology

Research Article
10.65520/erciyesfen.1791972

Imprint:
Volume: 42(1)
Year: 2026
Page: 221-238

Sedat Ozcanan[a*]
Ozgur Ozcan[b]
Zeynel Acar[c]

[a] Assoc. Prof., Şırnak University, sozcanan@sirnak.edu.tr
[b] Lec., Şırnak University, ozgurozcan@sirnak.edu.tr
[c] Civil Engineer , Şırnak University, zeynelacar2@gmail.com

* Corresponding Author

Received: 9/26/2025
Accepted: 2/9/2026

Citation:
Sedat Ozcanan, Ozgur Ozcan, Zeynel Acar, (2026). Investigation of the Effects of Concave and Convex Conditions of Steel Guardrails Installed Inside Curves on the Safety Parameters According to the EN 1317 Standard Using Finite Element Analysis. *Erciyes University Journal of Institue Of Science and Technology*, 42(1), 221-238. https://doi.org/10.65520/erciyesfen.*1791972*

Screened by iThenticate for Authors & Researchers

Investigation of the Effects of Concave and Convex Conditions of Steel Guardrails Installed Inside Curves on the Safety Parameters According to the EN 1317 Standard Using Finite Element Analysis

Abstract

Steel guardrail systems play a critical role in reducing injury severity during run-off-road crashes, especially on horizontal curves where accident rates are high. However, validation procedures defined in the EN 1317 standard are predominantly based on crash tests performed on straight road sections, and the influence of curved geometries is not sufficiently considered. This study numerically examines the effects of concave and convex horizontal curves on the safety performance of steel guardrails using finite element analysis (FEA). An EN 1317-compliant H1W4-A steel guardrail system was developed and validated under TB11 crash test conditions using LS-DYNA. The validated model was subsequently applied to concave and convex curve configurations with radii between 30 m and 210 m, resulting in a total of 14 numerical crash simulations. Key occupant safety parameters, namely the Acceleration Severity Index (ASI) and Theoretical Head Impact Velocity (THIV), together with structural performance measures such as working width (W) and exit angle (α), were systematically evaluated and compared with straight-road reference conditions. The results indicate that concave guardrails generally exhibit reduced impact severity, reflected by lower ASI and THIV values, compared to straight-road cases. In contrast, convex guardrails lead to higher and more critical safety indices, particularly at smaller radii. Although most configurations remain within EN 1317 limits, the R30 concave case exceeds allowable exit angle and working width thresholds. These findings highlight the necessity of incorporating road curvature effects into guardrail safety assessments.

Keywords: Horizontal curve, Guardrail, EN 1317, Crash test, Finite element analysis

Dönemeç İçine İnşa Edilen Çelik Otokorkulukların Konkav ve Konveks Durumlarının En 1317 Standardındaki Güvenlik Parametrelerine Etkisinin Sonlu Elemanlar Analizi ile Araştırılması

Öz

Çelik otokorkuluk sistemleri, özellikle kaza oranlarının yüksek olduğu yatay kurplarda meydana gelen yoldan çıkma kazalarında yaralanma şiddetinin azaltılmasında kritik bir rol oynamaktadır. Ancak EN 1317 standardında tanımlanan doğrulama prosedürleri ağırlıklı olarak düz yol kesitlerinde gerçekleştirilen çarpışma testlerine dayanmaktadır ve eğrisel yol geometrilerinin etkisi yeterince dikkate alınmamaktadır. Bu çalışmada, konkav ve konveks yatay kurpların çelik otokorkuluk sistemlerinin güvenlik

performansı üzerindeki etkileri sonlu elemanlar analizi (SEA) kullanılarak sayısal olarak incelenmiştir. EN 1317 ile uyumlu H1W4-A çelik otokorkuluk sistemi, TB11 çarpışma testi koşulları altında LS-DYNA yazılımı kullanılarak modellenmiş ve doğrulanmıştır. Doğrulanan model, 30 m ile 210 m arasında değişen yarıçaplara sahip konkav ve konveks kurp konfigürasyonlarına uyarlanmış ve toplam 14 adet sayısal çarpışma simülasyonu gerçekleştirilmiştir. Çalışmada, Hızlanma Şiddet İndeksi (ASI) ve Teorik Baş Çarpma Hızı (THIV) gibi yolcu güvenliğine ilişkin parametreler ile çalışma genişliği (W) ve çıkış açısı (α) gibi yapısal performans ölçütleri sistematik olarak değerlendirilmiş ve düz yol referans koşulları ile karşılaştırılmıştır. Elde edilen sonuçlar, konkav otokorkuluk sistemlerinin düz yol koşullarına kıyasla daha düşük ASI ve THIV değerleri sergileyerek daha az darbe şiddeti oluşturduğunu göstermektedir. Buna karşılık, konveks otokorkuluk sistemlerinin özellikle küçük yarıçaplı kurplarda daha yüksek ve kritik güvenlik seviyelerine yol açtığı belirlenmiştir. Çoğu konfigürasyon EN 1317 sınır değerleri içinde kalmasına rağmen, R30 konkav durumunda izin verilen çıkış açısı ve çalışma genişliği limitlerinin aşıldığı tespit edilmiştir. Bu bulgular, otokorkuluk güvenlik değerlendirmelerinde yol geometrisinin etkisinin mutlaka dikkate alınması gerektiğini ortaya koymaktadır.

Anahtar kelimeler: Yatay Kurp, Otokorkuluk, EN1317, Çarpışma testi, Sonlu elemanlar analizi

1. Introduction

Horizontal curves are one of the two key transition elements used in the geometric design of highways [1]. In 2020, there were 35,766 injury-related crashes on American highways resulting in 38,824 deaths, with more than 25% of these crashes occurring on horizontal curves [2, 3]. In Europe, where horizontal curves are more frequently employed on rural roads, 60% of crashes involve a single vehicle, and 32% of these occur on horizontal curves [4].

There are numerous studies and initiatives on active safety measures at horizontal curves—such as reducing vehicle skidding and installing curve warning signs—to improve road conditions and enhance safety [5, 6]. Nevertheless, the inevitably high incidence of single-vehicle crashes has made the use of barriers and other passive safety systems at horizontal curves increasingly important for reducing loss of life and property [7].

The impact severity level and structural performance analysis of a designed barrier are determined through full-scale crash tests conducted in accordance with criteria specified in standards, such as speed, impact angle, vehicle type, and weight [8–9]. Dynamic crash analysis can also be simulated and observed using nonlinear computer-aided programs based on the finite element (FE) method, offering savings in cost, time, and labor [10]. Finite element (FE) analyses have assumed an important role in barrier design and quality assessment due to their ease of application and repeatability [11]. When FE models are validated through full-scale crash tests [12, 13], they enable the successful execution of numerous crash scenarios [14, 15].

In recent years, within the framework of EN 1317 standards, numerous studies and investigations have been conducted on new and emerging topics related to roadside safety using FE analyses. Among the most noteworthy are the ANN metamodel [16], RBF-based barrier optimization [17], renewable hybrid barriers [18], the use of composite coatings on steel rails [19], and bollard systems [20]. Based on these studies, it is evident that FE analyses will continue to provide new perspectives on roadside safety in the coming years.

During a collision, there are numerous dummy- and vehicle-based criteria regulated under different standards for passenger safety. By employing methods such as full-scale crash tests [21] or validated simulations, it is possible to compare multiple criteria [22, 23] and gain insights into passenger safety. However, it should not be overlooked that, in calculating injury criteria such as ASI and THIV specified in EN 1317, different conditions and assumptions may lead to different results [24, 25, 26].

According to current standards, the validation of barriers depends on their successful completion of crash tests in which vehicles are impacted only against straight barriers. However, due to the geometric layout of the road at horizontal curves, convex and concave guardrail applications are frequently required. In such sharp curves, semi-rigid steel guardrails or steel cable systems should be

preferred because they can be bent to the desired shape according to the road's form and geometry [27]. To ensure roadside safety at horizontal curves under the criteria of EN 1317, several studies have been carried out, such as:

- safety analysis of cable barriers on convex curves with different radii [28, 29],
- performance of composite-coated steel barriers on concave curves [30, 31],
- crash test speed limits [32],
- investigation of the relationship between speed and ASI values for curved roadside safety barrier [33].

As in many of the above studies, it can be clearly seen that crash tests conducted on horizontal curves with large radii do not cause a significant change in safety performance compared to straight guardrails. On road sections with small curve radii, however, the extent to which the safety levels and structural performance of guardrails change during crashes remains a topic of interest. Another criterion is that the bending direction of the barrier may influence the interaction time between vehicles and the guardrail during impact, thereby affecting the impact severity level and working width. Unlike most existing studies, which either focus on straight road sections or investigate only a single curvature condition (concave or convex), the present work provides a systematic and direct comparison of concave and convex steel guardrail installations under identical EN 1317–TB11 impact conditions. By keeping the barrier type, test configuration, vehicle class, and evaluation criteria constant, the isolated influence of road curvature geometry on both occupant safety (ASI, THIV) and structural performance parameters (W, α) is quantified for the first time across a wide range of small radii. Furthermore, the results demonstrate that performance classes derived from straight-road crash tests may not be conservative for convex curves, where the impact severity can increase from ASI Level A to Level B. This finding reveals a critical limitation of current EN 1317-based safety assessments and constitutes the main originality and contribution of the study.

Based on these important considerations, this study aims to compare the safety and structural performance analyses of barriers with different small curve radii on convex and concave curves against those of straight barriers. In this context, an FE model of the EN 1317-TB11 test was first developed using the H1W4-A steel guardrail system and validated with full-scale crash test data. The barrier system was then designed as convex and concave for curve radii of 30, 60, 90, 120, 150, 180 and 210 m. A total of 14 TB11 FE simulations were performed, and the ASI–THIV values as well as the structural performance criteria were compared.

2. Material and Method

2.1. Occupancy safety criteria on EN 1317 standards

ASI and THIV are two fundamental criteria used in the EN 1317 standards to determine passenger safety. ASI is a parameter based on the acceleration exerted on passengers during a collision. As a function of time, ASI is calculated using the following equation.

$$ASI(t) = \left[\left(\frac{\bar{a}_x}{\hat{a}_x}\right)^2 + \left(\frac{\bar{a}_y}{\hat{a}_y}\right)^2 + \left(\frac{\bar{a}_z}{\hat{a}_z}\right)^2\right]^{0.5} \quad (1)$$

In this equation, the values $\bar{a}_x$, $\bar{a}_y$ ve $\bar{a}_z$ are the three-axis acceleration values recorded at δ =50 ms, which are calculated as in Equation (2) by accelerometers placed inside the vehicle.

$$\bar{a}_x = \frac{1}{\delta}\int_t^{t+\delta} a_x dt \,;\, \bar{a}_y = \frac{1}{\delta}\int_t^{t+\delta} a_y dt \,;\, \bar{a}_z = \frac{1}{\delta}\int_t^{t+\delta} a_z dt \quad (2)$$

The values $\hat{a}_x$, $\hat{a}_y$ ve $\hat{a}_z$ are the accepted limit acceleration values in the x, y, and z directions during a collision, assuming that the vehicle occupants are wearing seat belts. These values are defined

in terms of gravity as $\hat{a}_x$=12g, $\hat{a}_y$=9g ve $\hat{a}_z$=10g. The maximum value obtained from the ASI–time graph is designated as the final ASI value.

$$ASI = \max[ASI(t)] \tag{3}$$

ASI is a dimensionless quantity that only takes maximum values [34]. An increase in the ASI value indicates a higher likelihood of passenger injuries.

THIV is a measure of the theoretical velocity that a passenger's head inside the vehicle would reach upon striking a fixed surface within the vehicle during a collision. It assumes that the head velocity of the passengers is equal to the vehicle speed and is valid in cases where the vehicle does not overturn. In crash conditions, the standard distances of a passenger's head from a flat surface inside the vehicle are taken as 0.60 m in the x-direction and 0.30 m in the y-direction, respectively. Using these fundamental assumptions, the THIV value is calculated as a time-dependent function according to the following equation.

$$THIV = \left[{V_{head\ x}}^2(T) + {V_{head\ y}}^2(T)\right]^{0.5} \tag{4}$$

In the above equation, $V_{head\ x}$, ve $V_{head\ y}$ represent the head velocity values in the horizontal and vertical directions, respectively. The locations and orientations of the devices that need to be installed inside the vehicle for ASI and THIV measurements are shown in Figure 1. The relationship between the ASI and THIV limit values and the impact severity levels is presented in Table 1.

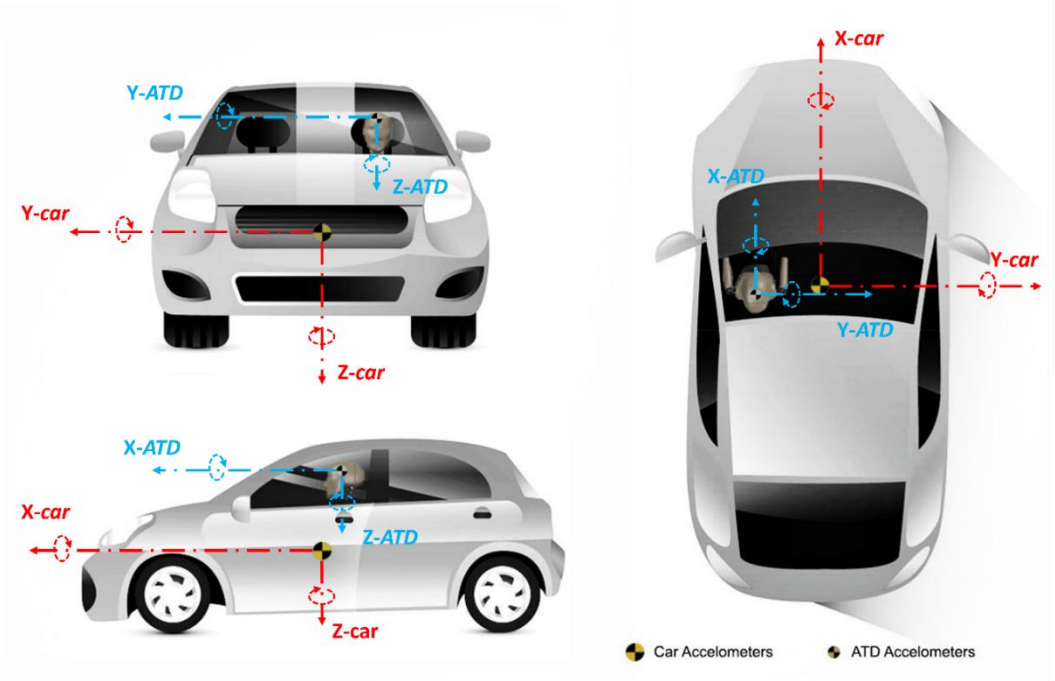

Figure 1. Accelerometer and dummy positions for ASI and THIV calculation [35]

Table 1. Impact severity levels [9]

Impact severity level	Index values		
A	ASI ≤ 1.0		
B	ASI ≤ 1.4	and	THIV ≤ 33 km/h
C	ASI ≤ 1.9		

2.2. Structural criteria on EN 1317 standards

In EN 1317 standards, there are several criteria used to evaluate the structural performance of barriers, such as working width (W), exit angle (a), and exit box. The working width (W) is defined as the maximum displacement occurring in the barrier after impact. The exit angle (α) is defined as the angle at which the vehicle departs from the barrier after impact. The exit box is the designated safe area determined from the exit point to prevent the vehicle from re-entering traffic after impact. The validity of the test depends on not exceeding the width (A) and length (B) values that constitute the exit box. The TB11 test conditions and structural performance criteria are shown in Figure 2. The limit values for the structural performance criteria in EN 1317 for the H1 guardrail system are provided in Table 2.

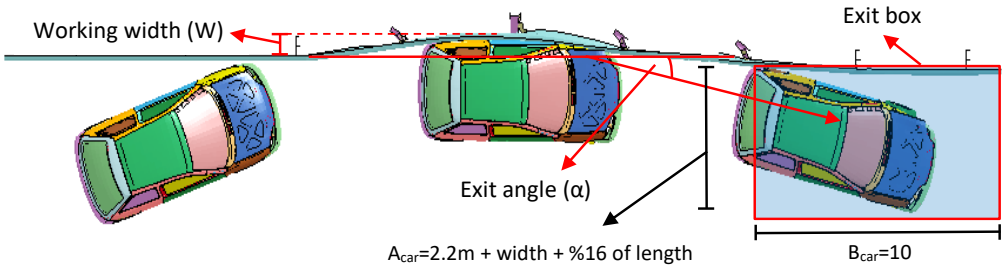

Figure 2. Illustration of crash test condition of EN1317 and exit box calculation [17,24]

Table 2. EN 1317 test evaluation criteria for H1 guardrail systems

System Type	Test	Working width (W) (m)	Exit box length(B)) (m)*	(width(A)x	Exit angle (a) (°)**
H1W4A	TB11	≤1.3	4.4x10		≤19

*Calculated based on EN1317/2
**Calculated based on exit box length

2.3. Virtual testing tolerance in European Norm (EN) 16303

The EN 16303 standards [36] include specific error tolerance values for each test criterion in the numerical modeling of the crash tests defined in EN 1317. These constraint values must be taken into account when simulating full-scale crash tests with numerical models. For a validation to be considered valid, these values must not be exceeded. The tolerance amounts for the investigated passenger safety criteria and structural performance criteria are presented in Table 3.

Table 3. EN 16303 virtual test tolerance for validation process [36]

Parameter	Tolerance
ASI	±0.1
THIV (km/h)	±3
W (m)	±0.1
Exit angle (°)	*

* Calculation and acceptance criterion is given in EN1317. Limit values are given in Table 2.

2.4. The Details and FE models of H1W4-A guardrail system and test vehicle

In this study, the H1W4-A type guardrail system, one of the most commonly used guardrail types, was selected. The symbols and classification categories used in the naming of the guardrail system are shown in Figure 3.

Figure 3. Symbol meanings of H1W4-A system [17-24]

The steel guardrail manufactured from S235JR steel consists of C-type posts and a W-beam. The geometric characteristics of the guardrail system and the FE model developed in LS-DYNA [37] are shown in Figure 4, while its technical specifications are presented in Table 4. In LS-DYNA, the rails and posts were defined as "Shell" elements, and the bolt connections as "Beam" elements, with the material properties given in Table 5. According to the EN 1317 standards [8,9], a steel guardrail system must remain structurally continuous during impact, and rupture of the rail is not permitted for a successful crash test. Consequently, the primary performance requirement is the controlled plastic deformation of the steel components without material failure. To realistically capture potential bolt failure mechanisms such as shear or tensile rupture, a rupture strain criterion was explicitly defined for the beam elements. Specifically, the failure strain was set to 0.15, and element erosion was activated once this strain threshold was exceeded. This value was selected based on commonly adopted practices in numerical crash simulations of roadside safety systems and ensures a realistic representation of bolt fracture without introducing excessive numerical instability. The guardrail model used in this study has been validated in previous studies [38, 39].

A uniform mesh size of 10 mm was employed for all guardrail components in order to ensure numerical consistency across all simulations. The finite element model was previously validated against full-scale TB11 crash test data and was found to comply with the EN 16303 tolerance requirements. Given that the objective of this study is a relative comparison of different curvature geometries rather than the prediction of absolute failure loads, a consistent meshing strategy was considered sufficient to isolate geometric effects. Nevertheless, it is acknowledged that further mesh sensitivity analyses could be conducted in future studies to investigate local stress and deformation characteristics in greater detail.

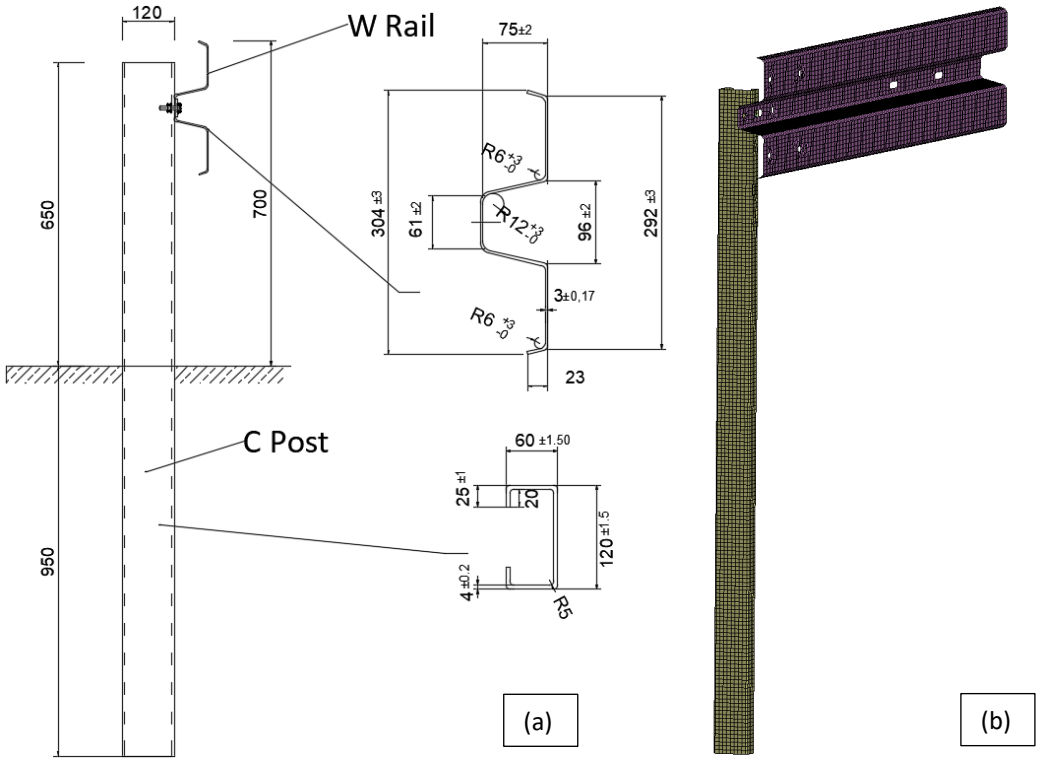

Figure 4. (a) H1W4 guardrail system details and (b) FE model of the design [38]

Table 4. Technical details of guardrail systems used in this study

System	Rail	Post	Material	Rail thickness (mm)	Post thickness (mm)
H1W4A	W	C120X60X20	S235JR	3.0	4.0

Table 5. Material definitions for guardrail system

Part	Material No	Material	Density (RO) (t/mm^3)	Elasticity Modulus (E) (MPa)	Poisson Rate (PR)	Yield (SIGY) (MPa)	Stress
Post Rail	MAT24	Piecewise Linear Plasticity	7,850e-09	2,050e+05	0,30	235	
M10 Bolt M16 Bolt	MAT98	Simplified Johnson Cook	1,000e-07	2,070e+05	0,28	---	

The mechanical response of guardrail posts embedded in the ground is highly dependent on soil conditions, with post rotation and deformation differing significantly between loose, medium-dense, and dense soils. In practical roadside applications and full-scale crash tests, guardrail systems are typically installed in selected fill materials or dense roadside soils. Previous experimental and numerical studies have consistently shown that, under dense soil conditions, the dominant post deformation occurs approximately 200 mm below the ground surface, primarily in the form of localized bending and rotation, while large-scale soil deformation plays a secondary role [7,12,16,17,24,35,38,39]. In the numerical model, the soil was not explicitly modeled as a continuum medium. Instead, the post–soil interaction was represented using an equivalent boundary condition approach. Guardrail posts were constrained at a depth of 200 mm below the ground surface, allowing rotation and deformation above this level while preventing rigid body motion. This modeling strategy reflects dense roadside soil conditions commonly assumed in full-scale crash tests and has been widely adopted in previous numerical studies to realistically capture post rotation behavior without

introducing excessive computational complexity.

The finite element model of the 900 kg vehicle [40] used in the TB11 test is shown in Figure 5.

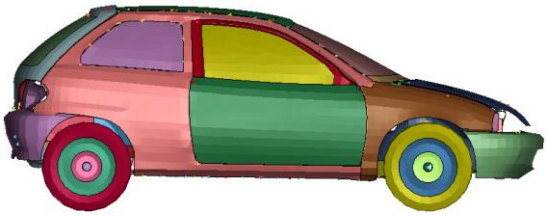

Figure 5. The FE models of vehicles used in TB11 test [40]

2.5. Validation of the FE models

As clearly stated in the title and objectives of this study, the focus is on the evaluation of safety parameters defined by EN 1317, rather than on the ultimate structural capacity of the barrier system under heavy vehicle impacts. Therefore, the use of the TB11 test was a deliberate and standard-consistent choice, as ASI and THIV can only be assessed using TB11-type light vehicle impacts within the EN 1317 framework. The validated finite element models (FEM) of the H1 guardrail and the vehicle were simulated in LS-DYNA by establishing the TB11 test conditions listed in Table 6, as specified in EN 1317. The crash test was conducted, and the finite element model (FEM) data were quantitatively compared with the full-scale crash test results [41] in Table 7.

Table 6. EN1317 test acceptance criteria for H1 guardrail systems [9]

System type	Test	Impact speed (km/h)	Impact angle (Θ) (°)	Total mass (kg)	Type of vehicle
H1	TB11	100	20	900	Car

Table 7. Comparison of data obtained from real tests [41] and FE models

Tests	Parameters	Real crash tests	FE models	Tolerance	Inside limits?
TB11	ASI	1.04	0.98	±0.1	Yes
	THIV (km/h)	32	31	±3	Yes

It is observed that the investigated parameters meet the limit values specified in the EN 1317 and EN 16303 standards, and that the developed finite element model (FEM) has been successfully validated. In addition, a qualitative comparison of the finite element model (FEM) with the full-scale crash test is presented in Figure 6. Based on the similarity between the two tests, it was concluded that the finite element model (FEM) is applicable for use in this study.

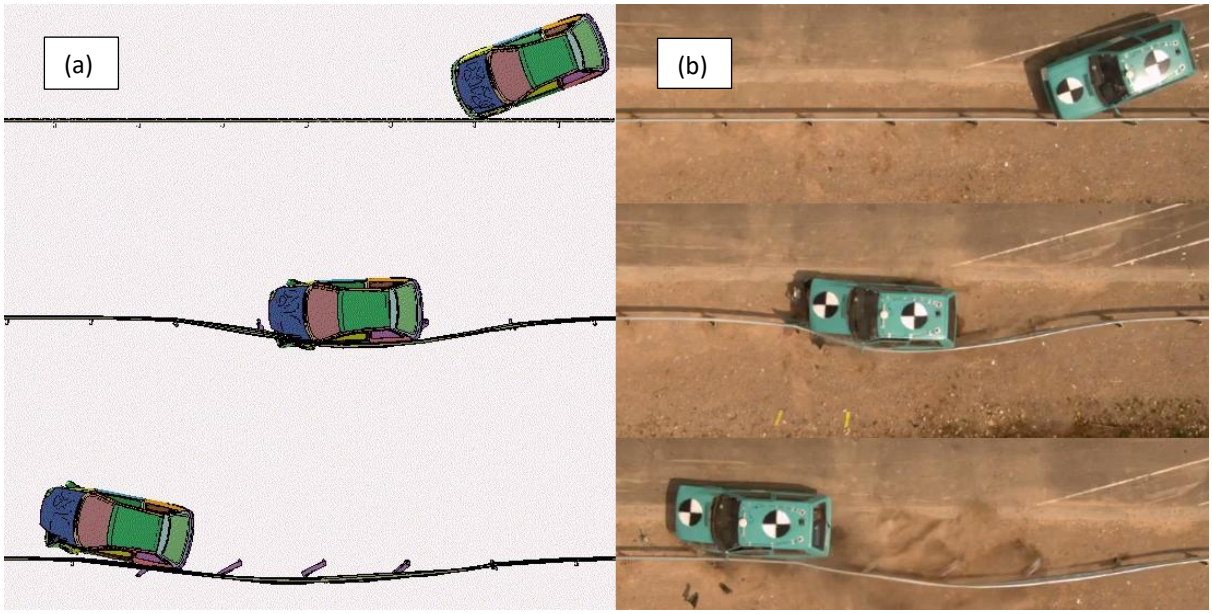

Figure 6. (a) FE model of TB11 (b) Real test of TB11 [38],[41]

The validated finite element model was extended to concave and convex geometries by applying geometric transformations to the barrier layout while preserving all material, contact, and numerical modelling parameters. Since the underlying physical interaction mechanisms remain unchanged, this approach allows the direct assessment of curvature effects without introducing additional modelling uncertainties. A uniform mesh density was adopted for all cases to ensure consistency, and the influence of curvature was evaluated on a relative basis.

3. Results

3.1. FE test setup

In line with the aim of the study, guardrails were modeled in AutoCAD 3D for all variations as convex and concave with curve radii of 30, 60, 90, 120, 150, 180, and 210 meters in three dimensions. The AutoCAD 3D drawings of the guardrails are presented in Figure 7. To enable these drawings to be opened in the LS-DYNA environment, the models created in AutoCAD 3D were saved in the "IGES" format.

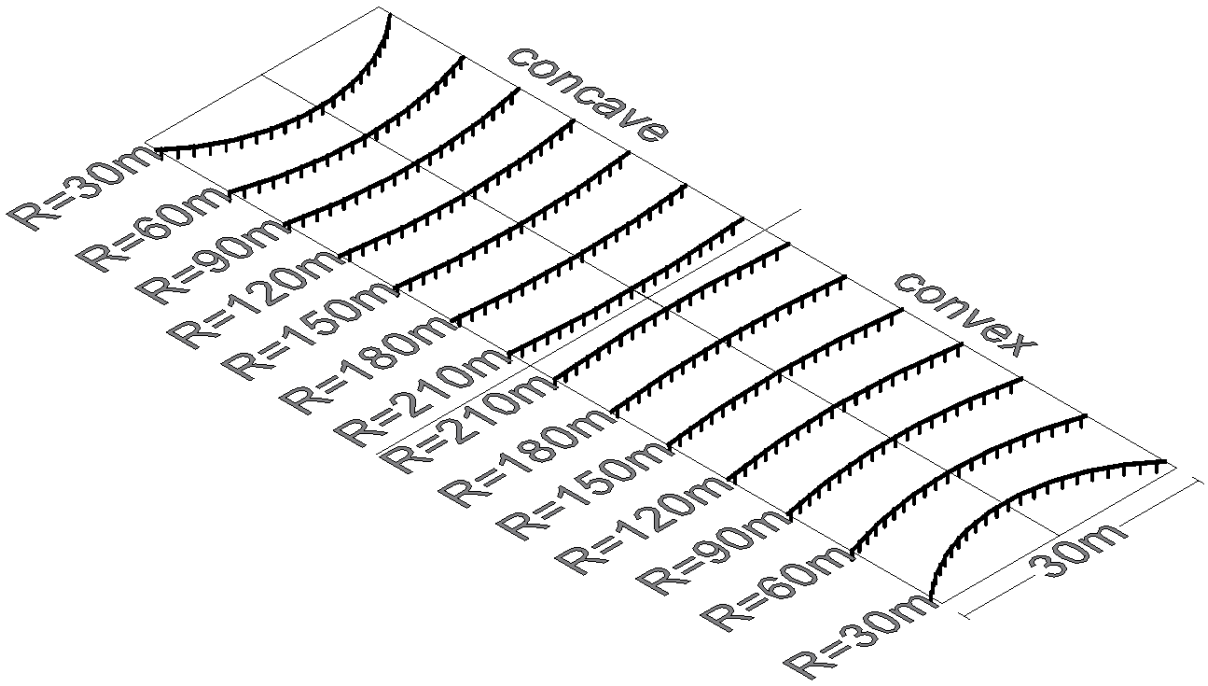

Figure 7. 3D AutoCAD drawings of all variations

The models opened in LS-DYNA in IGES format were initially meshed at 10 mm for all components, as shown in Figure 8(a). Subsequently, the basic properties of the models were defined by assigning part, section, and material characteristics. In Figure 8(b), each model is separated, and boundary conditions as well as control cards for the analysis are defined. Since an actual crash test was modeled in this study, the vehicle shown in Figure 5, possessing the specifications given in EN 1317, was added to all model variations as illustrated in Figure 8(c), and contact between the guardrail and the vehicle was defined. In addition, a planar ground surface was added to the model, shown in white in the figure. The TB11 test acceptance criteria provided in Table 6 were also defined in the model. The vehicle impact angle was set to 20°, and the speed to 100 km/h. As presented in Figure 8(c), the models were prepared for analysis.

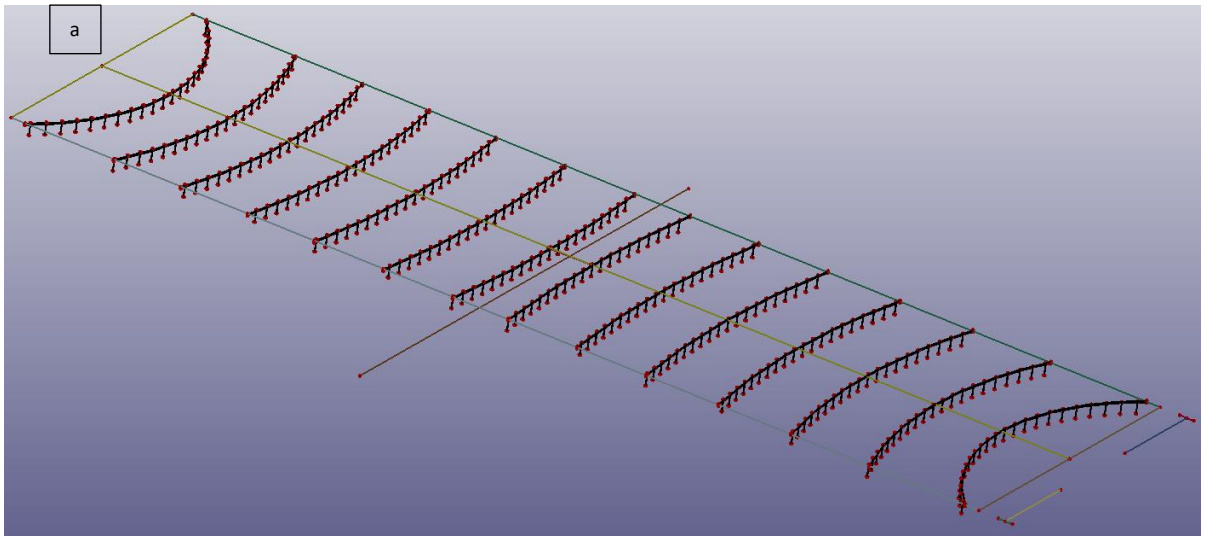

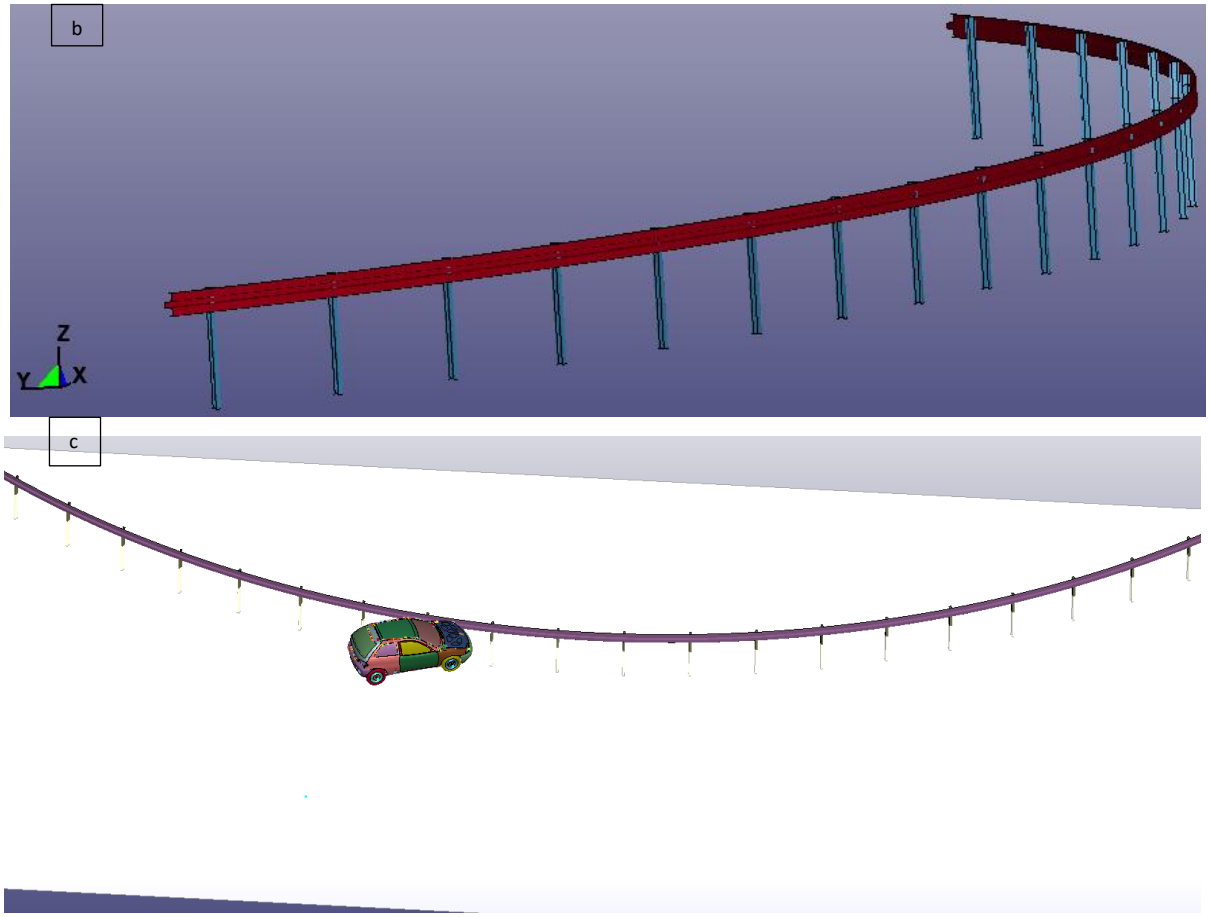

Figure 8. Finite elements model of guardrail variation in curve (a,b) and analysis setup (c)

3.2. FE Analysis and Results

Analyses were carried out for all variations with different convex and concave curvature radii, and the obtained results were calculated and evaluated within the methodology provided in Section 2. The real test data used for validating the numerical model will be employed for the comparison of these values. This real test pertains to a guardrail installed on a straight section of the road. The reference values obtained from the real test are taken as ASI = 1.04, THIV = 32.0 km/h, α = 9°, and W = 0.40 m, respectively [41]. The values such as ASI, THIV, α, and W obtained from the validated numerical crash tests for the concave-radius guardrails are presented in Table 8.

Table 8. Safety and performance values of the concave guardrail system

Concave radius	ASI	THIV (km/h)	Exit angle (a) (°)	Working width (W) (m)
R30	0.75	23.07	21	1.47
R60	0.81	24.92	10	0.88
R90	0.87	26.77	7	0.67
R120	0.85	26.15	7	0.58
R150	0.88	27.07	7	0.57
R180	0.93	28.61	6	0.53
R210	0.92	28.30	6	0.53
*R ∞	1.04	32.00	9	0.40

*References values

When examining the test results for the concave guardrail system, it can be seen from Figure 9 that the ASI values show a consistent increase with increasing curve radius but remain below the reference value. This indicates that the concave curvature geometry of the road reduces the ASI values to some extent. Similarly, THIV values were found to rise in parallel with ASI as the radius increases. As the concave radius grows, the working width (W) of the guardrail decreases, which makes the system behave more rigidly and consequently increases the ASI value. It can also be observed that as W decreases, the exit angle (α) also decreases. Considering all parameters together, concave guardrail systems appear to be safer than straight (R∞) systems in terms of vehicle and occupant safety. Therefore, it can be stated that guardrails developed and tested for straight road sections do not exhibit a weakness in terms of ASI impact severity in concave regions. However, it should be noted that for the R30 case only, the α and W values exceeded the limit values.

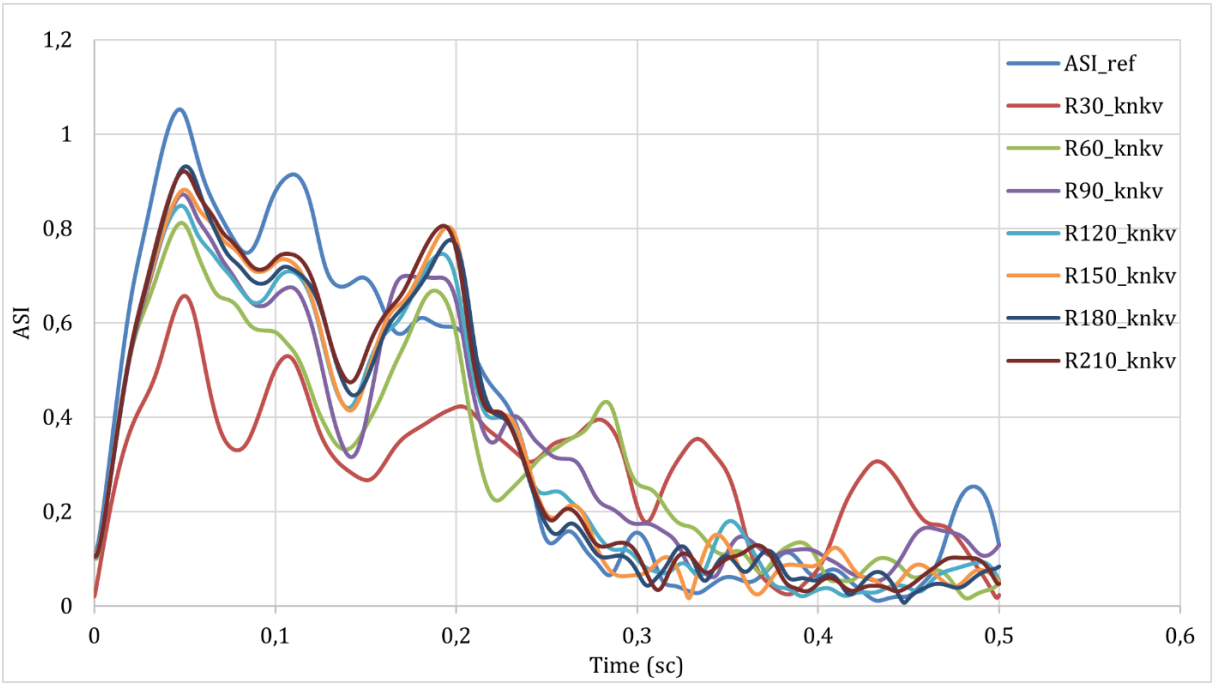

Figure 9. ASI performance of concave guardrails

When examining the test results for the convex guardrails presented in Table 9, it can be stated that the ASI, THIV, α, and W values increase proportionally with the radius. The noteworthy point here, as also shown in Figure 10, is that the ASI values at certain curvature radii exceeded the reference (R∞) value and reached the B impact severity level. As seen in the table, the α and W values remained within the critical limits. However, at R120, where the ASI impact severity reached its maximum, the THIV value exceeded the limit of 33.

Table 9. Safety and performance values of the convex guardrail system

Convex radius	ASI	THIV (km/h)	Exit angle (a) (°)	Working width (W) (m)
R30	0.89	27.38	5	0.22
R60	1.03	31.69	6	0.28
R90	1.05	32.30	7	0.32
R120	1.08	33.23	8	0.35
R150	1.03	31.69	8	0.35
R180	1.07	32.92	9	0.36
R210	1.01	31.07	9	0.36
R ∞	1.04	32.00	9	0.40

*References values

The primary reason why the overall results are not at a critical level is the use of a small vehicle in accordance with the TB11 standard during the tests. It is anticipated that tests conducted with larger vehicles could yield more critical outcomes in terms of safety parameters. When the curved road geometry is examined individually, it has been determined that the convex condition is more critical compared to the concave condition. This difference is thought to stem from the distinct mechanical behaviors inherent to concave and convex geometries. Therefore, it can be stated that, particularly for ASI impact severity and THIV, the level determined based on the straight section of the road may be inadequate for convex guardrails, unlike concave ones. The impact severity determined at the ASI A impact level on the straight section can drop to the B level under convex conditions. Considering also the α and W values of the R30 concave guardrail, it can be recommended that impact tests should be conducted not only for straight impacts but also by taking into account the curvatures constructed within the curve. This would help determine more reliable guardrail performance levels/classes both in terms of performance and safety.

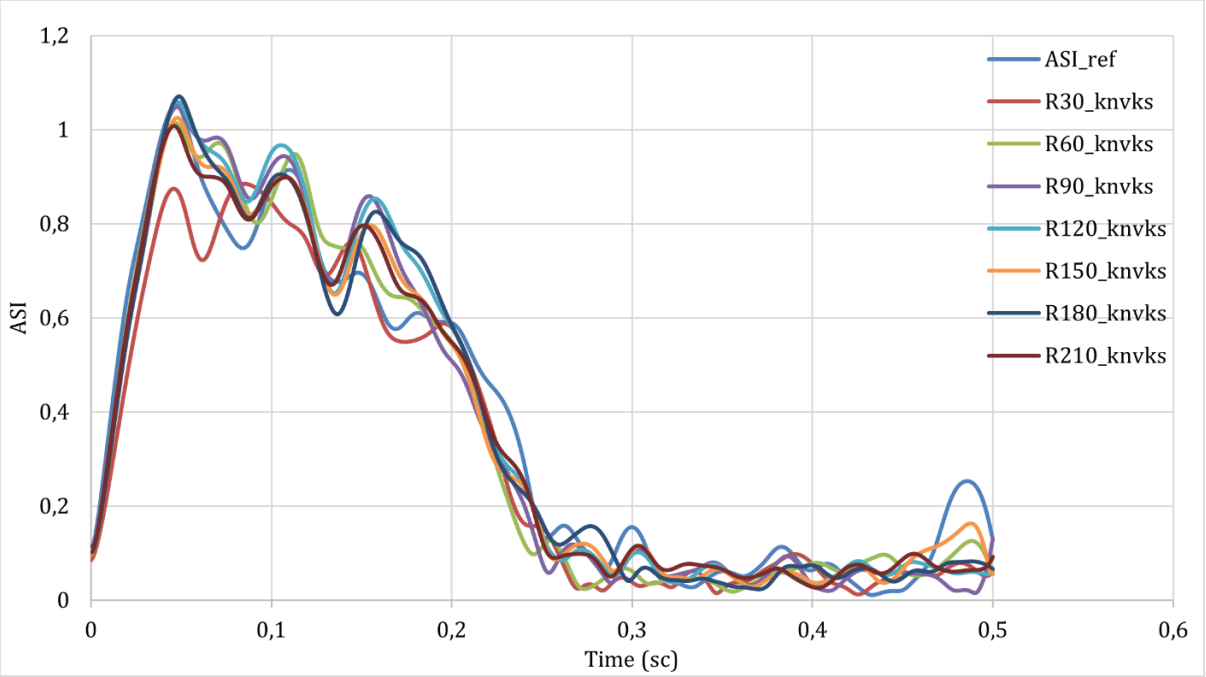

Figure 10. ASI performance of convex guardrails

In concave configurations, the vehicle interacts with the barrier over a longer effective contact length, which increases the interaction time and distributes impact forces more gradually along the guardrail. This leads to reduced peak accelerations and smoother deceleration profiles, resulting in lower ASI and THIV values. The concave geometry also promotes progressive post rotation and rail deformation, allowing the system to dissipate kinetic energy more efficiently.

In contrast, convex configurations cause a more abrupt vehicle–barrier interaction, characterized by a higher normal force component and a shorter contact duration. As a result, energy dissipation occurs over a reduced time interval, leading to higher peak accelerations and increased ASI and THIV values. This effect becomes more pronounced at smaller radii, where the localized and sudden engagement of the barrier limits its deformation capacity.

These mechanical differences explain why concave systems generally exhibit improved occupant safety performance, whereas convex systems represent more critical impact conditions.

4. Discussion and Conclusion

4.1. Comparison of the Obtained Results with the Literature

The results obtained in this study clearly indicate that the safety performance of steel guardrail systems installed on horizontal curves is strongly influenced by road geometry. When compared with existing studies in literature, the findings show both strong agreement and noteworthy differences that highlight the contribution of the present work. Most previous studies have evaluated crash performance and safety parameters primarily under straight road conditions, reporting that guardrails installed on curves with large radii do not exhibit significant deviations from straight-section behavior [28,29,32]. This observation is consistent with the results of the present study for both concave and convex systems with radii in the range of R150–R210, where ASI and THIV values remained close to the straight-road reference (R∞). However, the number of studies addressing small-radius horizontal curves remains limited. Klasztorny et al. [30,31] reported that, for concave curves, the vehicle–barrier interaction tends to occur over a longer duration, which can reduce impact severity. This mechanical behavior is directly supported by the present findings, as concave guardrails exhibited lower ASI and THIV values than straight-road conditions, particularly for radii between R60 and R210.

In contrast, studies focusing on convex curves suggest that this geometry may lead to more critical impact conditions. Wilde et al. [28] and Budzyński and Bruski [29] emphasized that vehicle–barrier contact on convex curves occurs more abruptly, resulting in higher impact severity. In close agreement with these observations, the present study found that ASI and THIV values for convex guardrails exceeded the straight-road reference and reached more critical levels, particularly in the R90–R120 radius range. Regarding structural performance parameters, previous research has generally reported that exit angle (α) and working width (W) are less sensitive to curvature effects than occupant safety parameters [30,33]. Similarly, in the present study, α and W values mostly remain within the standard limits. However, the R30 concave configuration exceeded the allowable limits for both α and W, indicating that very small-radius concave curves may also pose structural performance concerns. This finding represents an important addition to the existing literature.

4.2. Significance of the Findings and Contribution to Literature

In the existing literature, the safety performance of roadside barriers within the EN 1317 framework is predominantly assessed based on full-scale crash tests conducted on straight road sections, and the resulting performance classes are often generalized to all roadway geometries. The findings of the present study demonstrate that this assumption may be inadequate, particularly for convex horizontal curves. Specifically, an impact severity level classified as ASI Level A under straight-road conditions may escalate to Level B when the same barrier system is installed on a convex curve. This highlights a critical limitation of relying solely on straight section crash tests for safety evaluation. By explicitly comparing concave and convex geometries, this study fills an important gap in the literature and demonstrates that these two curvature conditions exhibit fundamentally different mechanical behaviors during vehicle–barrier interaction. The results clearly show that concave curves generally provide lower impact severity, whereas convex curves—especially those with small radii—represent more critical safety scenarios.

In conclusion, the present study demonstrates that:

- concave guardrails generally lead to reduced impact severity compared to straight-road conditions,
- convex guardrails can produce more critical ASI and THIV values, particularly at small radii, and
- road curvature geometry should be explicitly considered in both barrier design and crash test evaluation procedures.

These findings are expected to contribute to the development of safer roadside barrier designs

and may support future revisions of EN 1317 standards to better account for curved road geometries.

Implications:

The findings of this study have important practical implications for roadside safety design and assessment. The results indicate that performance classes derived from EN 1317 crash tests conducted on straight road sections may not be conservative for convex horizontal curves, where higher ASI and THIV values can occur. Therefore, road curvature should be explicitly considered as a design and evaluation parameter when selecting guardrail systems, particularly on small-radius convex curves.

Limitations:

Despite the valuable insights provided, this study has certain limitations. The analyses were limited to the TB11 test configuration using a 900 kg passenger car and a single H1W4-A steel guardrail system. Moreover, the results are based on validated finite element simulations and do not include full-scale crash tests on curved road sections. Soil conditions and installation variations were also idealized to ensure numerical stability and consistency.

Future Work:

Future studies should extend the present work by considering heavier vehicle classes such as TB32 and TB42, different barrier types and performance classes, and varying soil and installation conditions. Experimental crash tests on concave and convex curves would further support the numerical findings and could contribute to the refinement of current EN 1317 evaluation procedures. Such efforts may ultimately lead to safer and more geometry-sensitive roadside safety standards.

Peer-review: External, Independent.

Acknowledgements:
The authors declare that no specific financial support or institutional assistance was received for this research.

Declarations:

1. Statement of Originality:
The authors declare that this manuscript is an original work and has not been published previously, nor is it currently under consideration for publication elsewhere. All sources used in this study have been properly cited.

2. Author Contributions:
All authors contributed to the conception and design of the study. The authors participated in the literature review, methodology development, data analysis, and manuscript preparation. All authors reviewed and approved the final version of the manuscript.

3. Ethics approval:
This study does not involve human participants or animals; therefore, ethical approval was not required.

4. Funding/Support:
The authors received no financial support for the research, authorship, or publication of this article.

5. Competing Interests:
The authors declare that they have no competing financial interests or personal relationships that could have influenced the work reported in this paper.

6. GenAI Usage Statement:
During the preparation of this manuscript, generative artificial intelligence tools were used only for language editing and grammar improvement. The authors reviewed and edited the content and take full responsibility for the final manuscript.

7. Sustainable Development Goals:

REFERENCES

[1] Ma, Q., Yang, H., Wang, Z., Xie, K., Yang, D. 2020. Modeling crash risk of horizontal curves using large-scale auto-extracted roadway geometry data. Accident Analysis and Prevention, 144(2020), 105669. https://doi.org/10.1016/j.aap.2020.105669

[2] NHTSA. 2020. Fatality Analysis Reporting System. http://www-fars.nhtsa.dot.gov/Main/index.aspx (Access date: 09.04.2023).

[3] FHWA. 2019. Horizontal Curve Safety. https://safety.fhwa.dot.gov/roadway_dept/countermeasures/horicurves/ (Access date: 14.03.2022).

[4] European Transport Safety Council (ETSC). 2017. Reducing Deaths in Single Vehicle Collisions. PIN Flash Report No. 32. https://etsc.eu/wp-content/uploads/PIN_FLASH32-FINAL.pdf (Access date: 17.07.2024).

[5] Peng, J., Chu, L., Wang, T., Fwa, T. F. 2021. Analysis of vehicle skidding potential on horizontal curves. Accident Analysis and Prevention, 152(2021), 105960. https://doi.org/10.1016/j.aap.2020.105960

[6] Wood, J., Donnell, E. T. 2020. Empirical Bayes before-after evaluation of horizontal curve warning pavement markings on two-lane rural highways in Pennsylvania. Accident Analysis and Prevention, 146(2020), 105734. https://doi.org/10.1016/j.aap.2020.105734

[7] Atahan, A. O., Bonin, G., Karacasu, M. 2007. Development of a 30,000 kg heavy goods vehicle for LS-DYNA applications. International Journal of Heavy Vehicle Systems, 14(1)(2007), 1–19. https://doi.org/10.1504/IJHVS.2007.011929

[8] EN 1317-1:2010, Road restraint systems - Part 1: Terminology and general criteria for test methods. 2010.

[9] EN1317-2:2010, Road restraint systems - Part 2: Performance classes, impact test acceptance criteria and test methods for safety barriers including vehicle parapets Dispositifs. 2010.

[10] Sicking, D. L. 1995. Applications of simulation in design and analysis of roadside safety features. Transportation Research Circular, 435(1995).

[11] Ray, M. H. 1996. Repeatability of full-scale crash tests and criteria for validating simulation results. Transportation Research Record, 1528(1996), 155–160. https://doi.org/10.1177/0361198196152800117

[12] Atahan, A. O. 2002. Finite element simulation of a strong-post W-beam guardrail system. Simulation, 78(10)(2002), 587–599. https://doi.org/10.1177/0037549702078010001

[13] Ren, Z., Vesenjak, M. 2005. Computational and experimental crash analysis of the road safety barrier. Engineering Failure Analysis, 12(6)(2005), 963–973. https://doi.org/10.1016/j.engfailanal.2004.12.033

[14] Pawlak, M. 2016. The acceleration severity index in the impact of a vehicle against permanent road equipment support structures. Mechanics Research Communications, 77(2016), 21–28. https://doi.org/10.1016/j.mechrescom.2016.08.005

[15] Long, K., Gao, Z., Yuan, Q., Xiang, W., Hao, W. 2018. Safety evaluation for roadside crashes by vehicle–object collision simulation. Advances in Mechanical Engineering, 10(10)(2018), 1–12. https://doi.org/10.1177/1687814018805581

[16] Yılmaz, İ., Yelek, İ., Özcanan, S., Atahan, A. O., Hiekmann, J. M. 2021. Artificial neural network metamodeling-based design optimization of a continuous motorcyclists protection barrier system. Structural and Multidisciplinary Optimization, (2021). https://doi.org/10.1007/s00158-021-03080-1

[17] Ozcanan, S., Atahan, A. O. 2020. Radial basis function surrogate model-based optimization of guardrail post embedment depth in different soil conditions. Proceedings of the Institution of Mechanical Engineers, Part D: Journal of Automobile Engineering, 234(2–3)(2020), 739–761. https://doi.org/10.1177/0954407019848548

[18] Yumrutas, H. I., Ozcanan, S., Apak, M. Y. 2022. Experimental and numerical comparative crashworthiness analysis of innovative renewable hybrid barrier with conventional roadside barriers. International Journal of Crashworthiness, (2022), 1–17. https://doi.org/10.1080/13588265.2022.2075124

[19] Klasztorny, M. 2015. Rubber/foam/composite overlay onto guide B of barrier located on road bend. Archiwum Motoryzacji, 69(2015), 65–86.

[20] Apak, M. Y., et al. 2022. Finite element simulation and failure analysis of fixed bollard system according to the PAS 68:2013 standard. Engineering Failure Analysis, 135(2022), 106151. https://doi.org/10.1016/j.engfailanal.2022.106151

[21] Chell, J., Brandani, C. E., Frascetti, S., Chakraverty, J., Camomilla, V. 2019. Limitations of the European barrier crash testing regulation relating to occupant safety. Accident Analysis and Prevention, 133(2019), 105239. https://doi.org/10.1016/j.aap.2019.07.015

[22] Li, N., Fang, H., Zhang, C., Gutowski, M., Palta, E., Wang, Q. 2015. A numerical study of occupant responses and injuries in vehicular crashes into roadside barriers based on finite element simulations. Advances in Engineering Software, 90(2015), 22–40. https://doi.org/10.1016/j.advengsoft.2015.06.004

[23] D. Naish, D. A., Burbridge, A. 2015. Occupant severity prediction from simulation of small car impact with various concrete barrier profiles. International Journal of Crashworthiness, 20(5)(2015), 510–523. https://doi.org/10.1080/13588265.2015.1048177

[24] Ozcanan, S., Ozcan, O. 2022. Criteria inadequacy of the vehicles used for the calculation of safety parameters in the EN1317-TB11 test. Proceedings of the Institution of Mechanical Engineers, Part D: Journal of Automobile Engineering, (2022). https://doi.org/10.1177/09544070221115010

[25] Pachocki, L., Bruski, D., Burzyński, S., Chróścielewski, J., Wilde, K., Witkowski, W. 2018. On the influence of the acceleration recording time on the calculation of impact severity indexes. MATEC Web of Conferences, 219(2018), 03010. https://doi.org/10.1051/matecconf/201821903010

[26] Wilde, K., Burzyński, S., Bruski, D., Chróścielewski, J., Witkowski, W. 2017. TB11 test for short W-beam road barrier. 11th European LS-DYNA Conference, 2017, Salzburg.

[27] FHWA. 2016. Low-Cost Treatments for Horizontal Curve Safety. https://rosap.ntl.bts.gov/view/dot/50421 (Access date: 01.01.2018).

[28] Wilde, K., Bruski, D., Budzyński, M., Burzyński, S., Chróścielewski, J., Jamroz, K., Pachocki, Ł., Witkowski, W. 2020. Numerical analysis of TB32 crash tests for 4-cable guardrail barrier system installed on horizontal convex curves of road. International Journal of Nonlinear Sciences and Numerical Simulation, 21(1)(2020), 65–81. https://doi.org/10.1515/ijnsns-2018-0169

[29] Budzyński, M., Bruski, D. 2018. Assessing vehicle restraint systems on horizontal curves. MATEC Web of Conferences, 231(2018), 01004. https://doi.org/10.1051/matecconf/201823101004

[30] Klasztorny, M., Zielonka, K., Nycz, D. B., Posuniak, P., Romanowski, R. K. 2018. Experimental validation of simulated TB32 crash tests for SP-05/2 barrier on horizontal concave arc without and with composite overlay. Archives of Civil and Mechanical Engineering, 18(2)(2018), 339–355. https://doi.org/10.1016/j.acme.2017.07.007

[31] Klasztorny, M., Nycz, D. B., Zajac, K. P. 2019. Modelling and simulation of crash tests on curved barriers taking into account vehicle speed limits. Baltic Journal of Road and Bridge Engineering, 14(3)(2019), 304–325. https://doi.org/10.7250/bjrbe.2019-14.445

[32] Nycz, D. B. 2017. Influence of selected design parameters of the composite-foam cover rail on the course of the TB11 crash test of a road safety barrier forming a horizontal concave arc. Archiwum Motoryzacji, 76(2)(2017), 107–122. https://doi.org/10.14669/am.vol76.art5

[33] Nasution, R. P., Siregar, R. A., Fuad, K., Adom, A. H. 2009. The effect of ASI (Acceleration Severity Index) to different crash velocities. Proceedings of the International Conference on Applications and Design in Mechanical Engineering, (2009), 11–13.

[34] Shojaati, M. 2003. Correlation between injury risk and impact severity index ASI. 3rd Swiss Transport Research Conference, 2003, Switzerland, 19–21.

[35] Ozcanan, S., Özcan, Ö. 2025. Impact angle-based section design and optimization of the C post in order to improve the safety and structural performance of guardrails. Turkish Journal of Civil Engineering, 36(3)(2025), 93–108. https://doi.org/10.18400/tjce.1519835

[36] BS EN 16303:2020. Road restraint systems — Validation and verification process for the use of virtual testing in crash testing against vehicle restraint system. BSI Standards Publication, 2020.

[37] LSTC, 2019. A general-purpose dynamic finite element analysis program LS-DYNA version 971 user's manual. Livermore Software Technology Corporation, Livermore, California, USA, 2019.

[38] Ozcanan, S., Atahan, A. O. 2019. RBF surrogate model and EN1317 collision safety-based optimization of two guardrails. Structural and Multidisciplinary Optimization, 60(1)(2019), 343–362. https://doi.org/10.1007/s00158-019-02203-z

[39] Ozcanan, S., Atahan, A. O. 2021. Minimization of accident severity index in concrete barrier designs using an ensemble of radial basis function metamodel-based optimization. Optimization and Engineering, 22(1)(2021), 485–519. https://doi.org/10.1007/s11081-020-09522-x

[40] NCAC. 2008. Finite Element Model Archive. George Washington University FHWA/NHTSA National Crash Analysis Center. http://www.ncac.gwu.edu/vml/models.html (Access date: 12.11.2008).

[41] CSI, (2017). Crash testing of H1 and H2 guardrails systems. 0021\ME\HRB\17, Bollate, Italy.